THE UNIVERSITY *of* EDINBURGH

Edinburgh Research Explorer

Amplified spontaneous emission and collisional transfer from the f0(g)(+)(P-3(0)) ion-pair state of I-2

OPEN ACCESS

Amplified spontaneous emission and collisional transfer from the f0g+(3P0) ion-pair state of I2

Trevor Ridley, Kenneth P. Lawley, and Robert J. Donovan

Additional information on J. Chem. Phys.

Amplified spontaneous emission and collisional transfer from the $f0^+_g(^3P_0)$ ion-pair state of I_2

Trevor Ridley,[a] Kenneth P. Lawley, and Robert J. Donovan
School of Chemistry, The University of Edinburgh, West Mains Road, Edinburgh EH9 3JJ,
Scotland, United Kingdom

The work presented here extends previous studies of amplified spontaneous emission (ASE) between ion-pair (charge-transfer) states of I_2 and shows that ASE can occur between states correlating with different states of the cation, namely, $f0^+_g(^3P_0)$ and $D0^+_u(^3P_2)$, despite the smaller transition dipole moment between them. A value of 0.34 e Å is obtained for the transition dipole under experimental conditions where the $f0^+_g(^3P_0) \rightarrow D0^+_u(^3P_2)$ ASE is eliminated. No $F0^+_u(^3P_0) \leftarrow f0^+_g(^3P_0)$ ASE transfer is observed despite the combination of favorable Franck–Condon factors and transition dipoles. The $F0^+_u(^3P_0) \leftarrow f0^+_g(^3P_0)$ transfer is shown to be purely collisional and a propensity for transfers involving the smallest energy mismatch is observed. © *2009 American Institute of Physics.* [DOI: 10.1063/1.3098501]

I. INTRODUCTION

In most reported examples of amplified spontaneous emission (ASE) in small gas phase molecules at least one experimental parameter has to be extreme: long path lengths (1 m) for I_2 [$B0^+_u(ab) \rightarrow X0^+_g(aa)$, where a and b refer to the dissociation products, $I(^2P_{3/2})$ and $I(^2P_{1/2})$, respectively],[1] focused, high-power lasers (50 mJ/pulse) for H_2 (Ref. 2) or high pressures (>30 Torr) for CO (Ref. 3) and ND_3.[4] However, in two series of experiments it has been shown that the process can be readily observed without the need for any of these extreme conditions by using optical-optical double resonance (OODR) excitation. First, Tsukiyama and co-workers[5–8] used the technique to study NO. ASE was observed from transitions between Rydberg states where, like its atomic analog, it occurs for states of higher principal quantum number in the far infrared. Second, ASE was observed[9–12] between three pairs of ion-pair (IP) states of I_2, namely, $E0^+_g(^3P_2) \rightarrow D0^+_u(^3P_2)$, $\gamma 1_u(^3P_2) \rightarrow \beta 1_g(^3P_2)$, and $f'0^+_g(^1D_2) \rightarrow F'0^+_u(^1D_2)$, for which there is no atomic analog. The partners in each of these pairs of states are in the same tier, i.e., they correlate with I^+ in the same spectroscopic state ($^3P_2$ for the first two pairs and $^1D_2$ for the last pair). The energy separation of these g/u pairs near their equilibrium separation is small and the associated ASE again lies in the far infrared, typically at 200–800 cm^{-1}.

The threshold concentration for the ASE effect is given[13] by

$$N_c = N_{iv'} - N_{kv''} = 8\pi \Delta \nu / L\lambda^2 A_{iv'kv''}, \tag{1}$$

where $N_{iv'(kv'')}$ is the population of the upper (lower) level and L, $\Delta \nu$, and λ are the length of the active medium, the spectral width, and wavelength, respectively. $A_{iv'kv''}$, the Einstein coefficient, is given by

$$A_{iv'kv''} = 32\pi^3 \mu^2_{iv'kv''}/6\varepsilon_0 h\lambda^3 \tag{2}$$

and the transition dipole $\mu^2_{iv'kv''} \sim \mu_{ik}(R_e)^2 q_{v'v''}$ if the Franck–Condon factor (FCF) is introduced, hence

$$N_c = 3\varepsilon_0 h\Delta \nu \lambda / 2\pi^2 L\mu_{ik}(R_e)^2 q_{v'v''}. \tag{3}$$

If the line width, $\Delta \nu$ is equated with the Doppler width,

$$\Delta \nu = 7.16 \times 10^{-7} \nu \sqrt{(T/M)}, \tag{4}$$

where M is the molecular mass in atomic mass unit. Therefore,

$$N_c = 7.48 \times 10^{13} \sqrt{(T/M)}/L\mu_{ik}(R_e)^2 q_{v'v''}, \tag{5}$$

where $\mu_{ik}(R_e)$ is in e Å and L is in meters.

If the two states i and k are g/u partners in the same tier, $\mu_{ik}(R_e)$ will be very large and can approach that between almost degenerate Rydberg states of opposite parity. Since the spectroscopic constants of the partners in each g/u pair are very similar, the FCFs of close-lying vibrational levels will also be large—the FC matrix is almost diagonal in v, v'. From Eq. (5), these make the critical concentration for ASE relatively low. Substituting $\mu_{ik}(R_e) = 3.75$ e Å, typical of a charge-transfer process in IP states, gives $N_c = 5.3 \times 10^{15}$ molecules m^{-3} for a cell length of 10 cm and a FCF of 0.1. The necessary experimental conditions are then easy to obtain using OODR techniques even in the case of iodine with its low vapor pressure and large M. At room temperature the density of I_2 is 9×10^{21} molecules m^{-3} and the probability of finding a molecule in, say, $J=50$ is 2.3×10^{-2}. If the pump step ($B(v_2, J \pm 1) \leftarrow X(v_1, J)$) is saturated, and the probe step ($f(v_3, J$ or $J \pm 2) \leftarrow B(v_2, J \pm 1)$) is 1% efficient, a density of 10^{18} molecules m^{-3} in the IP state is achieved, three orders of magnitude above the critical level. Indeed, in addition to the transfer of excited state population between IP states by ASE, the highly directional emission itself from the IP state to the valence state carrying the largest transition dipole, e.g., ($E0^+_g(^3P_2) \rightarrow B0^+_u(ab)$) was

[a]Author to whom correspondence should be addressed. FAX: +44-131-6506453. Electronic mail: t.ridley@ed.ac.uk and tr01@staffmail.ed.ac.uk.

also readily observed in the visible at 425 nm. For this type of transition the transition dipole is an order of magnitude smaller than for transitions between g/u pairs of IP states. The characteristic time profile of the $E0_g^+(^3P_2) \rightarrow B0_u^+(ab)$ ASE emission has been measured by Nakano et al.[12]

When several channels of ASE originating in different electronic transitions are open, the decay is a competitive process and the dominant channel may well be decided by the availability of trigger photons once the threshold population has been reached. In all cases, the trigger photon may come from spontaneous emission. However, for IP→IP transitions in the same tier, these trigger photons may also come from black-body radiation as in NO.[8] In the case of IP →valence ASE, e.g., $E0_g^+(^3P_2) \rightarrow B0_u^+(ab)$, the robustness of the effect under widely different experimental conditions suggested that photons in the wings of the dye laser output used in the probe step may also be responsible.

In the present paper, we investigate whether ASE, or the consequences of it, originating from transitions between IP states of opposite g/u parity in *different* tiers can be observed under the experimental conditions used in OODR work. The transition dipoles will be considerably smaller than between IP states in the same tier and $\mu_{ik} \rightarrow 0$ as the IP separation $R \rightarrow \infty$, but very large FCFs (~ 1) can be found among adjacent vibrational levels in the initial and final states.

We have chosen the $f0_g^+(^3P_0) \rightarrow D0_u^+(^3P_2)$ transition, between states in the second and first tier, for investigation. The dominant ASE transition from the $f0_g^+(^3P_0)$ state would be expected to be its partner, the $F0_u^+(^3P_0)$ state. However, the electronic origin of the $f0_g^+(^3P_0)$ state lies below that of the $F0_u^+(^3P_0)$ state and consequently each v_f level lies below the vibrational level v_F with which it has the largest FC overlap (which occurs when $v_f = v_F$) and hence ASE between them cannot take place. Evidence, in the form of $D0_u^+(^3P_2) \rightarrow X0_g^+(aa)$ emission at 320 nm, for $f0_g^+(^3P_0) \rightarrow D0_u^+(^3P_2)$ ASE transfer, which would occur around 1700 nm, will be presented. The trigger for ASE in this case would be spontaneously emitted photons rather than black-body radiation or laser light. The excitation and emission pathways are illustrated in Fig. 1. The potential energy curves of the $X0_g^+(aa)$, $B0_u^+(ab)$, $D0_u^+(^3P_2)$, $f0_g^+(^3P_0)$, and $F0_u^+(^3P_0)$ states and the FCFs were calculated using the RKR1 and LEVELS programs of LeRoy[14,15] and the published molecular constants.[16–20]

While ASE itself may not be of direct spectroscopic interest, its occurrence, if unsuspected, can profoundly affect collisional energy transfer studies between the vibronic states connected by ASE, transition dipole measurements between such states, and lifetime measurements. It is then important to work under non-ASE conditions and the ease with which ASE can be generated may not have been recognized in the past. We illustrate this by a measurement of the $f0_g^+(^3P_0) \rightarrow D0_u^+(^3P_2)$ transition dipole. If, as we show, this is large enough to initiate ASE at excited state concentrations and with path lengths commonly used in OODR work, measurements of population transfer due solely to spontaneous emission without amplification must be made under controlled cell conditions.

In the course of the present work we observed $F0_u^+(^3P_0) \rightarrow X0_g^+(aa)$ emission following excitation of the
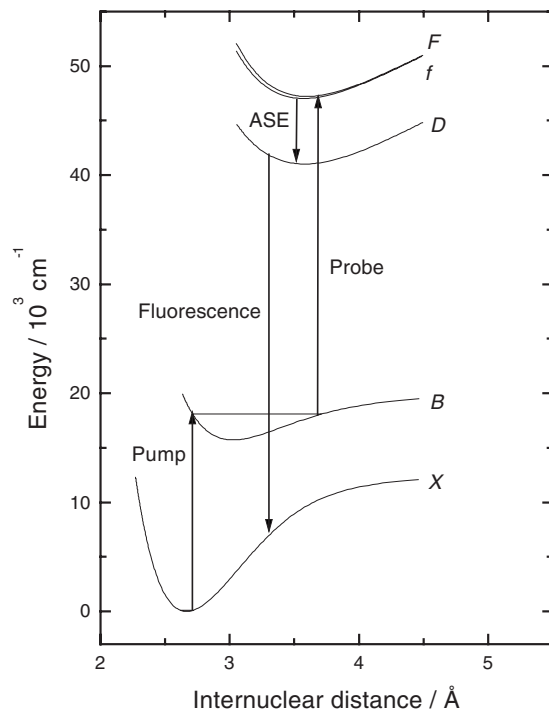

FIG. 1. The excitation and emission pathways involving $f0_g^+(^3P_0) \rightarrow D0_u^+(^3P_2)$ ASE.

$f0_g^+(^3P_0)$ state that indicated that the $F0_u^+(^3P_0) \leftarrow f0_g^+(^3P_0)$ transfer was via highly selective vibrational channels. Since, in two cases, the channels involved energy changes that were slightly endothermic, this cannot be excitation transfer by ASE. The mechanism is clearly collisional energy transfer between the two states of opposite g/u parity and we present some preliminary results for this transfer.

II. EXPERIMENTAL

A XeCl excimer laser (Lambda Physik EMG 201MSC) simultaneously pumped two Lambda Physik dye lasers; an FL 2002 operating with the dye C153 and an FL 3002E operating with the dye PTP (both ~ 3 mJ/pulse), provided the pump and probe photons, respectively. In all experiments known rotational levels with $J = 50 \pm 1$ of various vibrational levels of the $f0_g^+(^3P_0)$ state were excited. In the various excitation schemes, J was varied in order to ensure that the probe laser did not excite another rovibronic level in addition to the rovibrational level of the $f0_g^+(^3P_0)$ state of interest. The vibrational level in the intermediate $B0_u^+(ab)$ state was chosen so as to maximize the FCF for the probe stage.

The unfocused, counterpropagating, temporally overlapped pump and probe beams were directed through the glass sample cell that was fitted with Spectrosil quartz windows. The entrance/exit windows for the laser beams were at the Brewster angle. The cell was evacuated with a rotary backed turbo pump to a base pressure of 1×10^{-3} Torr that was measured by a 10 Torr MKS Baratron gauge connected directly to the cell. The solid I_2 was held in a side arm of the cell. Unless stated otherwise, the spectra were recorded with I_2 at its vapor pressure of ~ 0.23 Torr

The 15 cm long sample cell was positioned approximately halfway between two turning mirrors situated 4 m

apart. The pump and probe beams were aligned with two different geometries: (i) "parallel" where the beams completely overlap on both turning mirrors and (ii) "7°" where the beams cross in the emission collection region at an angle of 7°, the largest angle possible with the present cell. In effect, this reduces the path length L from 15 cm to <1 cm.

The 90° emission was dispersed by a Jobin-Yvon HRS2 (f/7, 0.6 m) monochromator and monitored by a Hammamatsu R928 photomultiplier tube. In order to collect 180° emission, a quartz plate was placed at 45° relative to the laser axis, directing ~10% of the combined pump laser beam and 180° emission into the spectrometer. Dispersed emission with $\lambda \leq 350$ nm was collected via a UG5 optical filter. While a lens was used to collect the 90° emission, the 180° emission was observed without any focusing optics.

The spectrometer slit width, i.e., the parameter that determines the resolution of the instrument remained constant throughout. The slit height was varied to ensure that the intensity of the emission gave a linear response from the photomultiplier. The output from the photomultiplier was processed by a Stanford Research SR250 gated integrator and stored on a personal computer.

Wavelength calibration of the dispersed fluorescence spectra was achieved by simultaneously recording the emission lines of a neon-filled lead hollow cathode lamp. The spectra used to determine the $f0_g^+(^3P_0) \rightarrow D0_u^+(^3P_2)$ transition dipole shown were corrected for the response function of the detection system in dimensions of power per unit wavelength. None of the spectra presented in the figures have been corrected in this way.

III. RESULTS

A. $f0_g^+(^3P_0) \rightarrow D0_u^+(^3P_2)$ ASE

1. $f0_g^+(^3P_0)$ ($v=0$)

An overview of the 90° emission observed in the range 250–350 nm following excitation of ($v=0$) of the $f0_g^+(^3P_0)$ state of I_2 via an OODR path involving ($v=17$) of the $B0_u^+(ab)$ state using parallel laser beams is shown in Fig. 2(a). Vibrational progressions from four electronic transitions, together with a bound-to-free continuum from a fifth, each with a Gaussian envelope characteristic of emission from ($v=0$), are observed. The strongest emission between 330 and 350 nm comes from the (parallel) $f0_g^+(^3P_0) \rightarrow B0_u^+(ab)$ transition. Weak (perpendicular) $f0_g^+(^3P_0) \rightarrow A1_u(aa)$ and $f0_g^+(^3P_0) \rightarrow C1_u(aa)$ direct emission from the initially excited state is also observed. In addition, weak $D0_u^+(^3P_2) \rightarrow X0_g^+(aa)$ and $F0_u^+(^3P_0) \rightarrow X0_g^+(aa)$ indirect emissions are also observed.

The $D0_u^+(^3P_2) \rightarrow X0_g^+(aa)$ emission must result, at least in part, as a consequence of $f0_g^+(^3P_0)$ ($v=0) \rightarrow D0_u^+(^3P_2)$ ($v=0$) ASE transfer. In an earlier paper[11] we showed that the magnitude of ASE can be controlled by partial misalignment of the laser beams, i.e., by varying L in Eq. (1). Nakano *et al.*[12] used a broadly similar approach to eliminating ASE by having the beams cross at 30°. In the present study we use beams crossing at 7° in an attempt to eliminate ASE. Expansions of the emission spectra in the range 286–327 nm recorded with parallel and 7° beams are shown in the lower
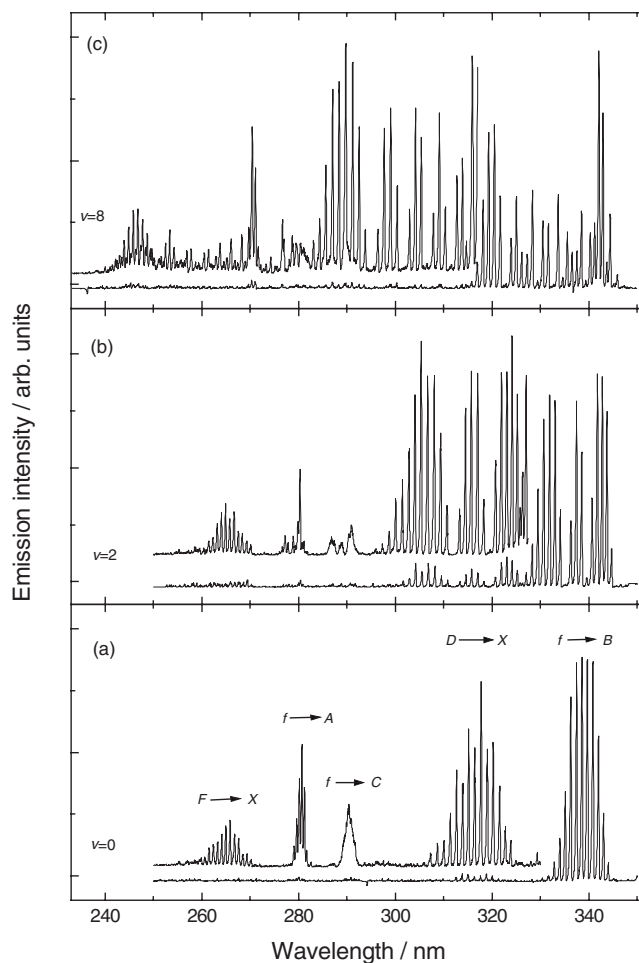

FIG. 2. Survey spectra of the 90° emission following the OODR excitation of (a) ($v=0$), (b) ($v=2$), and (c) ($v=8$) of the $f0_g^+(^3P_0)$ state of I_2 with parallel laser beams. The insets in each panel were recorded with increased spectrometer slit heights.

and upper traces of Fig. 3(a), respectively. The spectra are normalized to the intensity of the $f0_g^+(^3P_0) \rightarrow C1_u(aa)$ emission. The relative intensity of the $D0_u^+(^3P_2) \rightarrow X0_g^+(aa)$ emission in the spectrum recorded with 7° beams is greatly decreased, confirming that the $f0_g^+(^3P_0)$ ($v=0) \rightarrow D0_u^+(^3P_2)$ ($v=0$) transfer is predominantly by ASE when parallel beams are used.

2. $f0_g^+(^3P_0)$ ($v=2$)

An overview of the 90° emission observed in the range 250–350 nm following excitation of ($v=2$) of the $f0_g^+(^3P_0)$ state of I_2 via an OODR path involving ($v=21$) of the $B0_u^+(ab)$ state using parallel beams is shown in Fig. 2(b). $D0_u^+(^3P_2) \rightarrow X0_g^+(aa)$ emission resulting from $f0_g^+(^3P_0)$ ($v=2) \rightarrow D0_u^+(^3P_2)$ ($v=2$) ASE transfer is observed in the range 300–330 nm.

As before, the $f0_g^+(^3P_0)$ ($v=2) \rightarrow D0_u^+(^3P_2)$ ($v=2$) ASE can be eliminated by using 7° beams [Fig. 3(b)]. In addition, in the spectra recorded using 7° beams at three different I_2 pressures shown in Fig. 4(a), the intensity of the $D0_u^+(^3P_2) \rightarrow X0_g^+(aa)$ emission relative to that of the $f0_g^+(^3P_0) \rightarrow C1_u(aa)$ direct emission does not vary with I_2 pressure. Hence, the $D0_u^+(^3P_2) \rightarrow X0_g^+(aa)$ emission cannot be due to
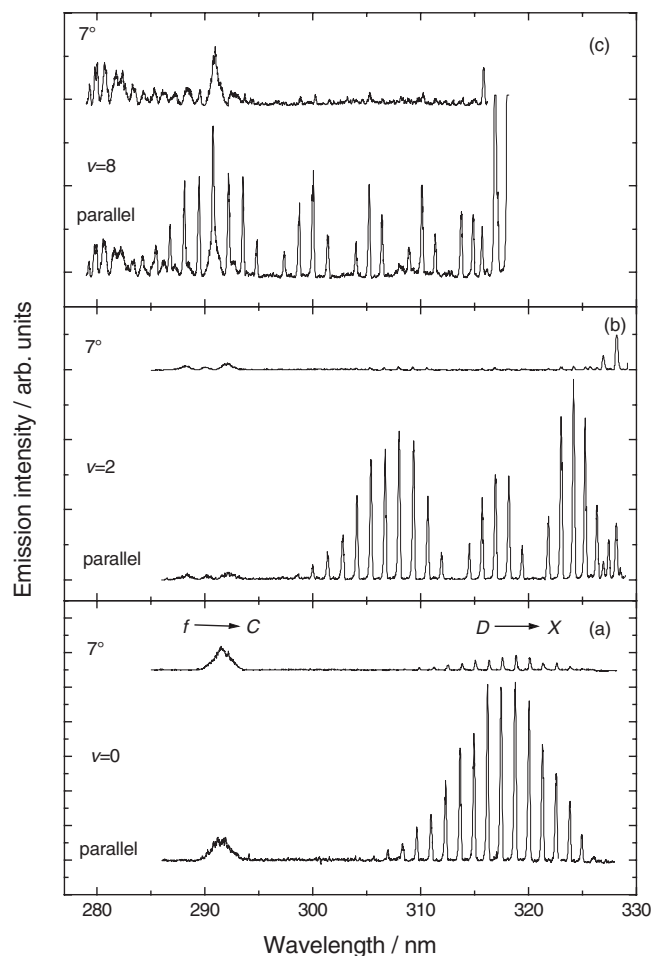
FIG. 3. The 90° $D0_u^+(^3P_2) \rightarrow X0_g^+(aa)$ emission following the OODR excitation of (a) ($v=0$), (b) ($v=2$), and (c) ($v=8$) of the $f0_g^+(^3P_0)$ state of I_2. In each panel, the lower and upper traces were recorded with parallel and 7° laser beams, respectively. The spectra are normalized to the intensity of the $f0_g^+(^3P_0) \rightarrow C1_u(aa)$ emission.

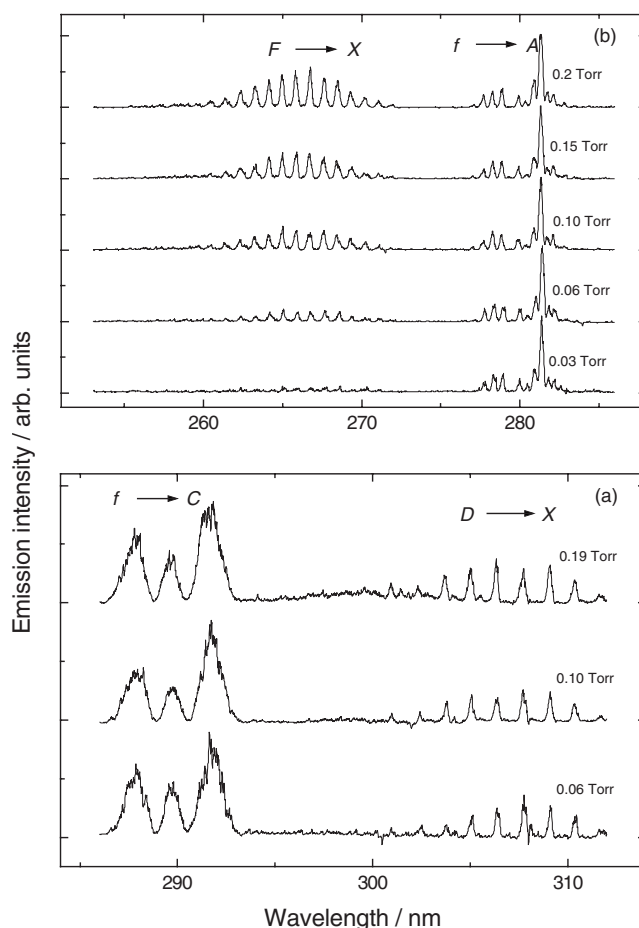

FIG. 4. The 90° $D0_u^+(^3P_2) \rightarrow X0_g^+(aa)$ and $F0_u^+(^3P_0) \rightarrow X0_g^+(aa)$ emissions following the OODR excitation of ($v=2$) of the $f0_g^+(^3P_0)$ state of I_2 recorded with 7° laser beams with various sample pressures: (a) $D0_u^+(^3P_2) \rightarrow X0_g^+(aa)$ normalized to the $f0_g^+(^3P_0) \rightarrow C1_u(aa)$ emission and (b) $F0_u^+(^3P_0) \rightarrow X0_g^+(aa)$ normalized to the $f0_g^+(^3P_0) \rightarrow A1_u(aa)$ emission.

$f0_g^+(^3P_0) \rightarrow D0_u^+(^3P_2))$ collisional transfer. Therefore, it is concluded that the $D0_u^+(^3P_2) \rightarrow X0_g^+(aa)$ emission observed in the 7° spectrum results purely from $f0_g^+(^3P_0)$ ($v=2$) $\rightarrow D0_u^+(^3P_2)$ ($v=2$) transfer by a spontaneous nonamplified optical transition, the precursor of the ASE transfer. We will use these experimental conditions in Sec. III to determine the $f0_g^+(^3P_0) \rightarrow D0_u^+(^3P_2)$ transition dipole.

In contrast, the intensity of the $F0_u^+(^3P_0) \rightarrow X0_g^+(aa)$ emission relative to that of the $f0_g^+(^3P_0) \rightarrow A1_u(aa)$ direct emission *does* vary with I_2 pressure as shown in the spectra in Fig. 4(b). Therefore, it is concluded that the $F0_u^+(^3P_0) \rightarrow X0_g^+(aa)$ emission results from $F0_u^+(^3P_0) \leftarrow f0_g^+(^3P_0)$ collisional transfer as proposed in earlier studies.[21,22] This transfer will be discussed further in Sec. IV.

3. $f0_g^+(^3P_0)$ ($v=8$)

An overview of the 90° emission observed in the range 235–350 nm following excitation of ($v=8$) of the $f0_g^+(^3P_0)$ state of I_2 using an OODR path involving ($v=29$) of the $B0_u^+(ab)$ state is shown in Fig. 2(c). $D0_u^+(^3P_2) \rightarrow X0_g^+(aa)$ emission resulting from $f0_g^+(^3P_0)$ ($v=8$) $\rightarrow D0_u^+(^3P_2)$ ($v=8$) ASE transfer is observed in the range 285–315 nm. Between 315 and 330 nm the high wavelength region of the

$D0_u^+(^3P_2) \rightarrow X0_g^+(aa)$ emission is concealed by the low wavelength region of the $f0_g^+(^3P_0) \rightarrow B0_u^+(ab)$ emission. As before, the $f0_g^+(^3P_0)$ ($v=8$) $\rightarrow D0_u^+(^3P_2)$ ($v=8$) ASE can be eliminated by using 7° beams [Fig. 3(c)].

4. $f0_g^+(^3P_0) \rightarrow B0_u^+(ab)$ emission

The 90° and 180° emissions from ($v=0$) of the $f0_g^+(^3P_0)$ state excited with parallel beams is shown in Figs. 5(b) and 5(d), respectively. The intensity distribution in the 90° spectrum reproduces the FC envelope, indicated by the stick spectrum in Fig. 5(a). In contrast, only the four most intense bands are seen in the 180° spectrum. A similar effect was observed in an earlier study on the $E0_g^+(^3P_2)$ state[9] and, as before, it is concluded that the 180° signal is predominantly directly observed ASE, in this case $f0_g^+(^3P_0) \rightarrow B0_u^+(ab)$, whereas the 90° signal is spontaneous fluorescence.

The 180° emission excited with 7° beams is shown in Fig. 5(c). It can be seen that this vibrational distribution resembles the 90° fluorescence shown in Fig. 5(b) much more closely than the 180° ASE shown in Fig. 5(d). This indicates that in the spectrum excited with 7° beams the 180° emission is almost entirely fluorescence rather than ASE. The three spectra in Fig. 5 are normalized to the intensity of the most intense band in each spectrum. However, the absolute inten-
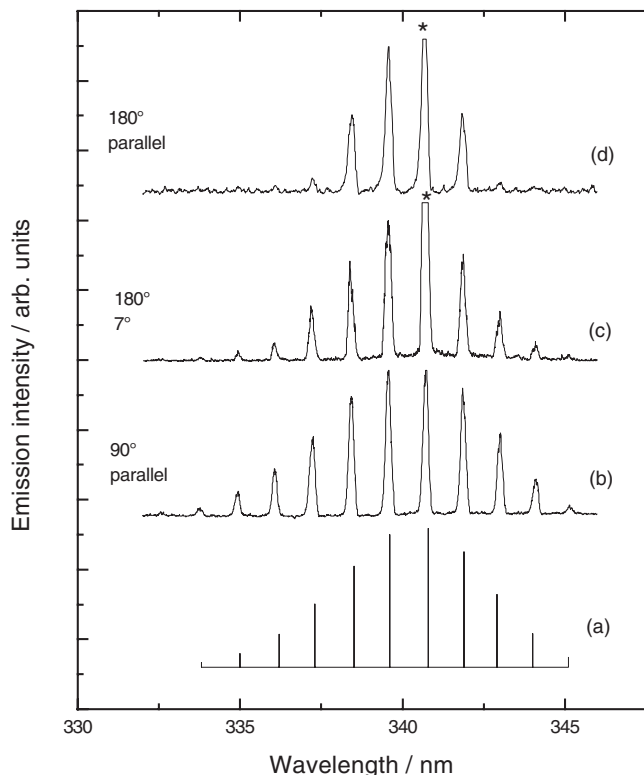
FIG. 5. The $f0_g^+(^3P_0) \rightarrow B0_u^+(ab)$ emission following excitation of $(v=0)$ of the $f0_g^+(^3P_0)$ state of I_2 with various geometries: (b) collected at 90° and excited with parallel beams, (c) collected at 180° and excited with 7° beams, and (d) collected at 180° and excited with parallel beams. The peaks indicated by a star contain some scattered probe laser light. A stick spectrum of the positions and raw FCFs for the $(J=50) \rightarrow (J=50)$ transitions is shown in (a). No frequency, transition dipole function or detector response function corrections have been applied to the intensities in the stick spectra.

sities of the spectra in (b) and (d) are at least an order of magnitude more intense than that in (c). Previous experiments[9] showed that with our experimental arrangement, for any given spontaneous fluorescence, 90° collection was approximately 30 times more efficient than 180° collection. This observation further indicates that in the spectrum excited with 7° beams the 180° emission is almost entirely spontaneous fluorescence. Hence, it is concluded that the 7° geometry is effective in greatly reducing $f0_g^+(^3P_0) \rightarrow B0_u^+(ab)$ ASE as well as eliminating $f0_g^+(^3P_0) \rightarrow D0_u^+(^3P_2)$ ASE.

B. Measurement of the $f0_g^+(^3P_0) \rightarrow D0_u^+(^3P_2)$ transition dipole

In order to determine the $f0_g^+(^3P_0) \rightarrow D0_u^+(^3P_2)$ transition dipole, the integrated fluorescence intensities of the various emission systems from the $f0_g^+(^3P_0)$ state, namely, $f0_g^+(^3P_0) \rightarrow B0_u^+(ab)$, $f0_g^+(^3P_0) \rightarrow A1_u(aa)$, $f0_g^+(^3P_0) \rightarrow C1_u(aa)$, and $f0_g^+(^3P_0) \rightarrow D0_u^+(^3P_2)$, have to be obtained. I_{ik}, the integrated fluorescence intensity of the transition $i \rightarrow k$ relative to the total fluorescence, is then obtained from

$$I_{ik} = S_{ik}/\Sigma_k S_{ik}, \tag{6}$$

where S_{ik}, in photons s^{-1}, is the integrated fluorescence intensity for each electronic transition.

S_{ik} values for the first three systems were measured directly but that for the fourth system had to be determined indirectly by initially measuring S_{ik} for $D0_u^+(^3P_2) \rightarrow X0_g^+(aa)$, S_{DX}. If the $D0_u^+(^3P_2)$ state population is created solely by $f0_g^+(^3P_0) \rightarrow D0_u^+(^3P_2)$ fluorescence without any collisional or ASE transfer, as described in Sec. I, and if the $D0_u^+(^3P_2)$ state is not collisionally quenched, $S_{fD} = S_{DX}/I_{DX}$. In an earlier study,[23] I_{DX} was reported to be 0.89.

Rewriting Eq. (2), $\mu_{ik}(R_e)$, in e Å, is given by

$$\mu_{ik}(R_e)^2 = A_{iv'kv''}\nu^3 \times 7.24 \times 10^{-6}, \tag{7}$$

where ν, in wave numbers, is the median frequency of the transition and $A_{iv'kv''}$ is given by

$$A_{iv'kv''} = I_{ik}/\tau_i, \tag{8}$$

where τ_i is the lifetime of the upper state.

S_{ik} values for each electronic transition $i \rightarrow k$ were determined by first recording spectra of the various emission systems from $(v=0)$ of the $f0_g^+(^3P_0)$ state and integrating each with respect to wavelength. The values obtained were then corrected to: (i) account for the response function of the detection system (in dimensions of power per unit wavelength) and (ii) convert to units of photons s^{-1}. For both corrections, a single value that applies to the wavelength centroid of the narrow emission system resulting from the low upper state vibrational level was used, e.g., 341 nm for $f0_g^+(^3P_0) \rightarrow B0_u^+(ab)$.

There is an inherent problem associated with accurately measuring the relative integrated intensities of two emission systems that differ by two orders of magnitude. The magnitude of the fluorescence collected must be large enough for the signal-to-noise ratio to be such that an accurate integrated intensity can be measured, while ensuring that it is not too large for partial saturation of the detection system to occur for the strong emission. In order to circumvent this problem, the three weak emission systems, together with the weaker part of the $f0_g^+(^3P_0) \rightarrow B0_u^+(ab)$ emission, namely, to $(v=9-11)$ of the lower state, were recorded with good signal-to-noise levels and ratios of the integrated intensities determined. The percentage contribution that the $(v=9-11)$ bands make to the total $f0_g^+(^3P_0) \rightarrow B0_u^+(ab)$ emission was then calculated from the FCFs, corrected for the wavelength, transition dipole, and response function dependencies.

The resultant S_{ik} values were used to obtain I_{ik} for each system and these are presented in Table I. $A_{iv'kv''}$ and $\mu_{ik}(R_e)$ for each transition were then obtained from Eqs. (7) and (8) using a fluorescent lifetime of 13.7 ns,[24] and these are also presented in Table I. The errors in I_{ik} and $\mu_{ik}(R_e)$ for the weak emissions are estimated to be $\sim \pm 20\%$ and $\pm 10\%$, respectively. The I_{ik} values for $f0_g^+(^3P_0) \rightarrow A1_u(aa)$ and $f0_g^+(^3P_0) \rightarrow C1_u(aa)$ are approximately one third of those reported previously[23] for these weak transitions and replace those erroneous values.

The S_{ik} value for the $f0_g^+(^3P_0) \rightarrow D0_u^+(^3P_2)$ transition was obtained by dividing the value for $D0_u^+(^3P_2) \rightarrow X0_g^+(aa)$ by 0.89.[23] However, this value is an upper limit as it has been subsequently shown[10] that there is some $D0_u^+(^3P_2) \rightarrow 0_g^+(bb)$ emission, for which the transition dipole is unknown, that was not included in the original calculation. If a value for the

TABLE I. Analysis of the integrated fluorescence from the $f0_g^+(^3P_0)$ IP state. The values for the $D0_u^+(^3P_2)$ state were obtained by inference, assuming a certain model for the $f0_g^+(^3P_0)$ state as described in the text.

Lower state	$\lambda/$nm	Wave number/cm^{-1}	I_{ik}	$A_{iv'kv''}/10^5$ s^{-1}	$\mu_{ik}(R_e)/$e Å
$A1_u(aa)$	282	35 461	0.003 91	2.85	0.030
$C1_u(aa)$	292	34 247	0.004 01	2.93	0.032
$B0_u^+(ab)$	341	29 326	0.990	723	0.63
$D0_u^+(^3P_2)$	1667	5999	0.002 42	1.77	0.34

dipole of the $D0_u^+(^3P_2) \rightarrow 0_g^+(bb)$ transition relative to that for the $D0_u^+(^3P_2) \rightarrow X0_g^+(aa)$ transition is assumed, the ratio of the integrated fluorescence intensities can then be obtained by correcting for the wavelengths of the two systems, 740 and 318 nm, respectively. For example, if it is assumed that the dipoles for the $D0_u^+(^3P_2) \rightarrow 0_g^+(bb)$ and $D0_u^+(^3P_2) \rightarrow X0_g^+(aa)$ transitions are equal, this corresponds to the $D0_u^+(^3P_2) \rightarrow X0_g^+(aa)$ percentage contribution decreasing from 89% to 83%. This, in turn, increases the value of μ for the $f0_g^+(^3P_0) \rightarrow D0_u^+(^3P_2)$ transition from 0.34 to 0.35 e Å, i.e., the value is fairly insensitive to the magnitude of the $D0_u^+(^3P_2) \rightarrow 0_g^+(bb)$ emission.

We have obtained a value of 0.34 ± 0.05 e Å for the $f0_g^+(^3P_0) \rightarrow D0_u^+(^3P_2)$ transition dipole. This is surprisingly high, although still much less than the giant transition dipole for g/u transitions within the same tier of IP states ($\sim$3.6 e Å). However, 0.34 e Å is just over half the magnitude of the dipoles for the $E0_g^+(^3P_2) \rightarrow B0_u^+(ab)$ and $f0_g^+(^3P_0) \rightarrow B0_u^+(ab)$ IP$\rightarrow$valence transitions where ASE has been observed directly and this would explain why $f0_g^+(^3P_0) \rightarrow D0_u^+(^3P_2)$ ASE can be induced under favorable experimental conditions. Had the transition dipole been determined from spectra recorded in the presence of ASE, i.e., from the spectrum recorded with parallel beams [the lower trace of Fig. 3(a)] rather than from the spectrum recorded with 7° beams [the upper trace of Fig. 3(a)], it would have been approximately three times too large.

C. $F0_u^+(^3P_0) \leftarrow f0_g^+(^3P_0)$ transfer

1. ASE transfer

Expansions of the $F0_u^+(^3P_0) \rightarrow X0_g^+(aa)$ emission spectra in the range 255–275 nm following excitation of ($v=2$) of the $f0_g^+(^3P_0)$ state recorded with parallel and 7° beams are shown in the lower and upper traces of Fig. 6(a), respectively. The spectra are normalized to the intensity of the $f0_g^+(^3P_0) \rightarrow A1_u(aa)$ emission (not shown). The spectra are dominated by emission from $F0_u^+(^3P_0)$ ($v=0$). The relative intensity and the vibrational distribution in the $F0_u^+(^3P_0) \rightarrow X0_g^+(aa)$ emission in the two spectra is essentially the same indicating that there is no appreciable $F0_u^+(^3P_0) \leftarrow f0_g^+(^3P_0)$ ASE transfer. Under identical conditions, the $f0_g^+(^3P_0) \rightarrow D0_u^+(^3P_2)$ ASE is eliminated in the 7° beam spectrum as shown in Fig. 2(b).

The absence of $F0_u^+(^3P_0)$ ($v=0$) $\leftarrow f0_g^+(^3P_0)$ ($v=2$) ASE transfer is not surprising even though the route is now open as $f0_g^+(^3P_0)$ ($v=2$) lies 20 cm^{-1} above $F0_u^+(^3P_0)$ ($v=0$). While the transition dipole (3.6 e Å) for the transition is large, the FCF is very small (2×10^{-3}). When Eq. (5) is simplified to

$$N_c \propto 1/\mu_{ik}(R_e)^2 q_{v'v''} \qquad (9)$$

the value of the denominator (0.026) is still much smaller than that for the $f0_g^+(^3P_0)$ ($v=2$)$\rightarrow D0_u^+(^3P_2)$ ($v=2$) transition (0.13) where ASE can be induced.

Expansions of the emission spectra in the range 275–235 nm, normalized to the intensity of the $f0_g^+(^3P_0) \rightarrow A1_u(aa)$ emission, following excitation of ($v=8$) of the $f0_g^+(^3P_0)$ state recorded with parallel and 7° beams, are shown in the lower and upper traces of Fig. 6(b), respectively. The spectra are dominated by emission from $F0_u^+(^3P_0)$ ($v=7$). As for ($v=2$), the relative intensity and the vibrational distribution in the $F0_u^+(^3P_0) \rightarrow X0_g^+(aa)$ emission in the two spectra are essentially the same indicating that there is no appreciable $F0_u^+(^3P_0) \leftarrow f0_g^+(^3P_0)$ ASE transfer.

The absence of $F0_u^+(^3P_0)$ ($v=6$) $\leftarrow f0_g^+(^3P_0)$ ($v=8$) ASE
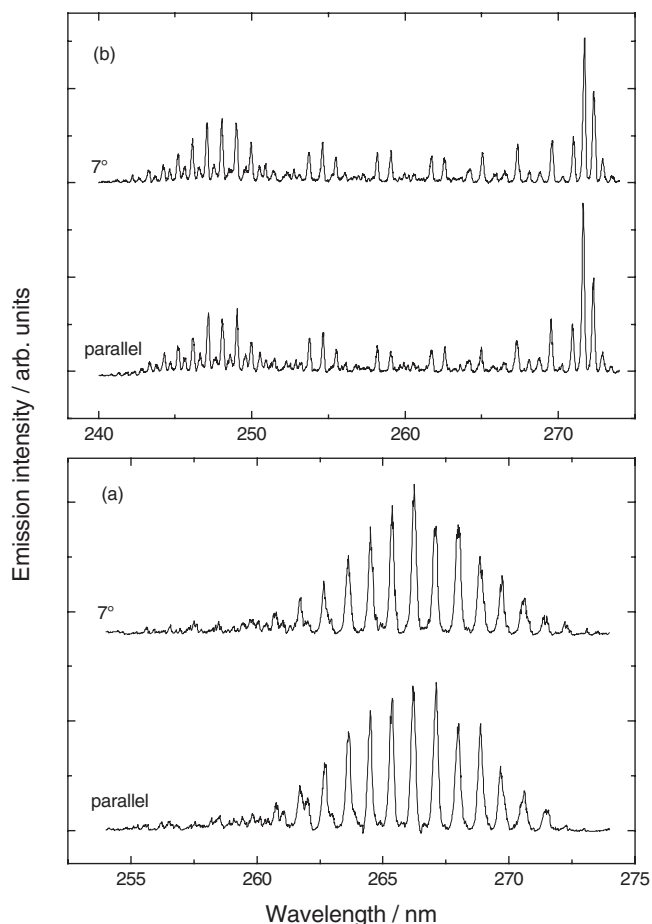

FIG. 6. The 90° $F0_u^+(^3P_0) \rightarrow X0_g^+(aa)$ emission spectra in the range 275–250 nm following excitation of (a) ($v=2$) and (b) ($v=8$) of the $f0_g^+(^3P_0)$ state recorded with parallel and 7° beams. The spectra are normalized to the intensity of the $f0_g^+(^3P_0) \rightarrow A1_u(aa)$ emission (not shown).

transfer is surprising as $f0_g^+(^3P_0)$ ($v=8$) lies 72 cm^{-1} above $F0_u^+(^3P_0)$ ($v=6$). The FCF for this transition is larger (3.4 $\times 10^{-2}$) making the value of the denominator in Eq. (9), (0.44), greater than that for the $f0_g^+(^3P_0)$ ($v=8$)$\rightarrow D0_u^+(^3P_2)$ ($v=8$) transition where ASE can be induced.

Although the critical concentration for $F0_u^+(^3P_0)$ $\leftarrow f0_g^+(^3P_0)$ ASE can probably be achieved, the absence of ASE points to the crucial role of trigger photons. The smaller FCFs for even the most favorable $F0_u^+(^3P_0)\leftarrow f0_g^+(^3P_0)$, q_{86} $=0.034$, $q_{20}=0.0021$ compared with $q_{88}=0.92$, $q_{22}=0.97$ for the competing $f0_g^+(^3P_0)\rightarrow D0_u^+(^3P_2)$ transitions, combined with the very different fluorescent wavelengths means that the Einstein A coefficients, and hence the rates of spontaneous emission of trigger photons for the $F0_u^+(^3P_0)$ $\leftarrow f0_g^+(^3P_0)$ transitions are very small compared with those for the $f0_g^+(^3P_0)\rightarrow D0_u^+(^3P_2)$ transitions. The only way in which an $F0_u^+(^3P_0)\leftarrow f0_g^+(^3P_0)$ transition could exhibit ASE would be through efficient triggering by black-body photons, the rate of which is nA_{Ff}, where n is the photon occupation number at ν_{Ff}. For the most favorable case of $F(v=0)$ $\leftarrow f(v=2)$, for which $\nu_{Ff}=20$ cm^{-1}, $n\sim 10$, but nA_{Ff} is still only $1.1\times 10^{-8}A_{fd}$, in spite of the more favorable intratier transition dipole.

2. Transfer by collisions with ground state I_2

As no evidence for $F0_u^+(^3P_0)\leftarrow f0_g^+(^3P_0)$ ASE is observed, it is concluded that the transfer is due to collisions with $I_2 X0_g^+(aa)$. Stick spectra of the positions and raw FCFs for the $(J=50)\rightarrow (J=50)$ transitions of the various $F0_u^+(^3P_0)\rightarrow X0_g^+(aa)$ vibronic bands observed following excitation of $f0_g^+(^3P_0)$ ($v=2$ and 8) using 7° beams are shown in Figs. 7(a) and 7(b), respectively. No frequency, transition dipole function, or detector response function corrections have been applied to the intensities in the stick spectra since in both cases an estimate of the relative concentrations of the $F0_u^+(^3P_0)$ state levels can easily be made from a narrow wavelength region at the blue end of the emission system where the component bands become resolved. Thus, we estimate the relative concentrations of $F0_u^+(^3P_0)$ ($v=0$):($v=1$):($v=2$) to be 10:1.5:1 following excitation of $f0_g^+(^3P_0)$ ($v=2$) and of $F0_u^+(^3P_0)$ ($v=6$):($v=7$):($v=8$) to be 1:10:2.5 following excitation of $f0_g^+(^3P_0)$ ($v=8$).

The propensity for $F0_u^+(^3P_0)$ ($v=0$)$\leftarrow f0_g^+(^3P_0)$ ($v=0$) [Fig. 2(a)] is not surprising as the final state level lies 190 cm^{-1} above the initial level ($\Delta E=190$ cm^{-1}), hence transfer to higher levels would involve an even greater increase in energy. The dominant transfer from $f0_g^+(^3P_0)$ ($v=2$) goes to $F0_u^+(^3P_0)$ ($v=0$), the level with the smallest energy mismatch ($\Delta E=-20$ cm^{-1}) but with a small FCF (2 $\times 10^{-3}$) in preference to going to $F0_u^+(^3P_0)$ ($v=2$), the level with the largest FCF (0.85) and an energy mismatch of ΔE $=170$ cm^{-1}. The dominant transfer from $f0_g^+(^3P_0)$ ($v=8$) goes to $F0_u^+(^3P_0)$ ($v=7$), as before, the level with the smallest energy mismatch ($\Delta E=20$ cm^{-1}) in preference both to $F0_u^+(^3P_0)$ ($v=8$), the level with the largest FCF and ΔE $=110$ cm^{-1}, and $F0_u^+(^3P_0)$ ($v=6$), a transfer involving a loss of energy ($\Delta E=-70$ cm^{-1}).

Akopyan et al.[25,26] studied the collisional transfer from
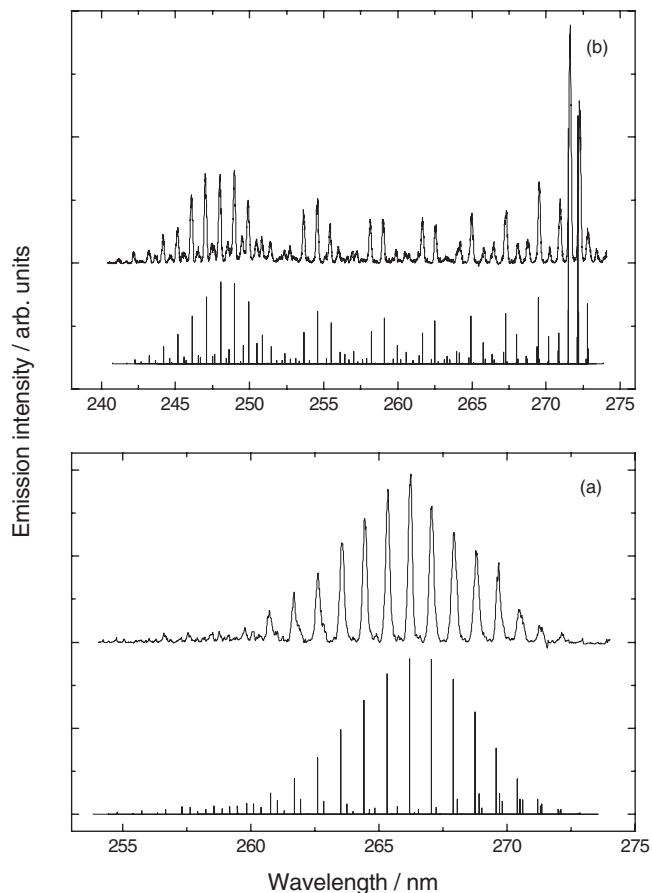

FIG. 7. The 90° $F0_u^+(^3P_0)\rightarrow X0_g^+(aa)$ emission spectra in the range 275–250 nm following excitation of (a) ($v=2$) and (b) ($v=8$) of the $f0_g^+(^3P_0)$ state. The stick spectra show the positions and raw FCFs for the $(J=50)\rightarrow(J=50)$ transitions without any frequency, transition dipole function, or detector response function corrections. The relative concentrations shown are (a) ($v=0$):($v=1$):($v=2$) 10:1.5:1 and (b) ($v=6$):($v=7$):($v=8$) 1:10:2.5.

($v=8$–19) of the $f0_g^+(^3P_0)$ state by $I_2 X0_g^+(aa)$. Following excitation of $f0_g^+(^3P_0)$ ($v=8$, $J=55$) they observed the strongest emission from $F0_u^+(^3P_0)$ ($v=6$, 7 and 8) in the approximate ratios 1:2.2:2; ratios that are significantly different to those observed in the present study, i.e., 1:10:2.5. This intriguing observation merits more extensive investigation.

IV. CONCLUSIONS

Direct $f0_g^+(^3P_0)\rightarrow B0_u^+(ab)$ ASE has been observed that can be largely suppressed by reducing the length of the active medium, i.e., by having the pump and probe beams at 7° to each other. In addition, $f0_g^+(^3P_0)\rightarrow D0_u^+(^3P_2)$ ASE from ($v=0,2,8$) has been observed indirectly by collecting subsequent $D0_u^+(^3P_2)\rightarrow X0_g^+(aa)$ emission. This ASE can be totally suppressed in the same way. A value of 0.34 e Å has been obtained for the $f0_g^+(^3P_0)\rightarrow D0_u^+(^3P_2)$ transition dipole using 7° beams. The value is similar to those for the strongest IP $\rightarrow$ valence transitions and explains why ASE can be induced.

No $F0_u^+(^3P_0)\leftarrow f0_g^+(^3P_0)$ ASE transfer from ($v=0,2,8$) has been observed, despite the combination of FCFs and transition dipoles apparently being favorable in some cases. It has been proposed that this is due to a low abundance of trigger photons for the transitions. Highly selective vibrational channels for $F0_u^+(^3P_0)\leftarrow f0_g^+(^3P_0)$ collision transfer by

I_2 $X0_g^+(aa)$ have been observed in which transfer from (v =2 and 8) goes predominantly to (v=0 and 7), respectively, showing a propensity for transfers involving the smallest energy mismatch.

[1] J. W. Glessner and S. J. Davis, J. Appl. Phys. **73**, 2672 (1993).

[2] U. Czarnetzki and H. F. Döbele, Phys. Rev. A **44**, 7530 (1991).

[3] U. Westblom, S. Agrup, M. Aldén, H. M. Hertz, and J. E. M. Goldsmith, Appl. Phys. B: Lasers Opt. **50**, 487 (1990).

[4] Y. Ogi and K. Tsukiyama, Chem. Phys. **303**, 271 (2004).

[5] J. Ishii, K. Uehara, and K. Tsukiyama, J. Chem. Phys. **104**, 499 (1996).

[6] Y. Ogi, M. Takahashi, K. Tsukiyama, and R. Bersohn, Chem. Phys. **255**, 379 (2000).

[7] Y. Ogi, A. Sakoda, H. Mutoh, H. Taki, and K. Tsukiyama, Chem. Phys. **271**, 215 (2001).

[8] Y. Ogi, J. Ando, M. Nemoto, M. Fujii, K. Tono, and K. Tsukiyama, Chem. Phys. Lett. **436**, 303 (2007).

[9] V. A. Alekseev, T. Ridley, K. P. Lawley, and R. J. Donovan, Chem. Phys. Lett. **443**, 34 (2007).

[10] T. Ridley, K. P. Lawley, R. J. Donovan, and V. A. Alekseev, Phys. Chem. Chem. Phys. **9**, 5885 (2007).

[11] T. Ridley, K. P. Lawley, and R. J. Donovan, Chem. Phys. **348**, 227 (2008).

[12] Y. Nakano, H. Fujiwara, M. Fukushima, and T. Ishiwata, J. Chem. Phys. **128**, 164320 (2008).

[13] L. Allen and G. I. Peters, Phys. Rev. A **8**, 2031 (1973).

[14] R. J. LeRoy, University of Waterloo Chemical Physics Research Report No. CP-425 (1992).

[15] R. J. Le Roy, University of Waterloo Chemical Physics Research Report No. CP-655 (2002).

[16] R. Martin, R. Bacis, S. Churassy, and J. Vergès, J. Mol. Spectrosc. **116**, 71 (1986).

[17] P. Luc, J. Mol. Spectrosc. **80**, 41 (1980).

[18] J. Tellinghuisen, J. Mol. Spectrosc. **217**, 212 (2003).

[19] J. S. Hickmann, C. R. M. de Oliveira, and R. E. Francke, J. Mol. Spectrosc. **127**, 556 (1988).

[20] T. Ishiwata, T. Kusayanagi, T. Hara, and I. Tanaka, J. Mol. Spectrosc. **119**, 337 (1986).

[21] H. P. Grieneisen and R. E. Francke, Chem. Phys. Lett. **88**, 585 (1982).

[22] U. Heemann, H. Knöckel, and E. Tiemann, Chem. Phys. Lett. **90**, 17 (1982).

[23] K. P. Lawley, P. J. Jewsbury, T. Ridley, P. R. R. Langridge-Smith, and R. J. Donovan, Mol. Phys. **75**, 811 (1992).

[24] P. J. Jewsbury, K. P. Lawley, T. Ridley, F. F. Al Adel, P. R. R. Langridge-Smith, and R. J. Donovan, Chem. Phys. **151**, 103 (1991).

[25] M. E. Akopyan, I. Y. Chinkova, T. V. Fedorova, S. A. Poretsky, and A. M. Pravilov, Chem. Phys. **302**, 61 (2004).

[26] M. E. Akopyan, I. Y. Novikova, S. A. Poretsky, A. M. Pravilov, A. G. Smolin, T. V. Tscherbul, and A. A. Buchachenko, J. Chem. Phys. **122**, 204318 (2005).